Inorganic Chemistry

Article

pubs.acs.org/IC

Solid-State Synthesis of Molybdenum and Tungsten Porphyrins and Aerial Oxidation of Coordinated Benzenethiolate to Benzenesulfonate

Goutam Nandi and Sabyasachi Sarkar*

Department of Chemistry, Indian Institute of Technology Kanpur, Kanpur 208016, India

Supporting Information

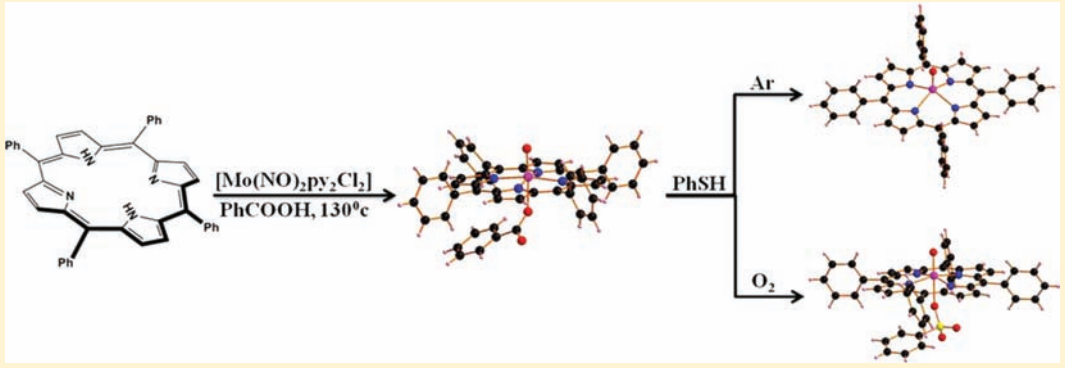

ABSTRACT: A new route is developed for the synthesis of molybdenum and tungsten porphyrins using $[M(NO)_2py_2Cl_2]$ (M = Mo, W) as the metal source and TPP (dianion of 5,10,15,20-*meso*-tetraphenylporphyrin) in the benzoic acid melt. Complexes $[Mo^{V}O(TPP)(OOCPh)]$ (**1**) and $[W^{V}O(TPP)(OOCPh)]$ (**2**) are isolated in almost quantitative yield. These are characterized by single-crystal X-ray structure analysis, electron paramagnetic resonance, electronic and IR spectroscopy, and magnetic moment measurements. Benzenethiol substitutes for $PhCOO^{-}$ in **1**, forming an intermediate thiolato complex that responds to the intramolecular redox reaction across the Mo^{V}−SPh bond to yield $[Mo^{IV}O(TPP)]$ (**3**). Under an excess of benzenethiol, PhS^{-} is coordinated to the vacant site in **3**, which under aerial oxidation is oxidized to benzenesulfonate to form $[Mo^{V}O(TPP)(O_3SPh)]$ (**4**). **2** undergoes similar aerial oxidation chemistry albeit slowly.

INTRODUCTION

Metalloporphyrins are important for diverse photocatalytic reactions ranging from solar energy trapping to photodynamic therapy.[1,2] Normally, metalloporphyrins are synthesized in two steps, where the free-base porphyrins are synthesized first, followed by the metalation reaction.[3] A one-pot general synthesis of metalloporphyrins was introduced by us to save time and to improve the yield.[4] However, the synthesis of tungsten porphyrin is difficult. $K_3W_2C1_9$ as a source material has been used to synthesize tungsten porphyrin in high yield under prolonged refluxing with a free-base porphyrin in benzonitrile.[5] The conventional method for the preparation of tungsten or molybdenum porphyrin involves refluxing of the corresponding hexacarbonyl and porphyrin in a high-boiling solvent.[6,7] Similar methodology is also employed for the incorporation of these two metals in a closely related macrocycle corrole.[8] In some cases, molybdenum oxychloride ($MoOCl_3$) or molybdenum pentachloride ($MoCl_5$) is also used as the metal source.[9] However, either these reactions are very slow or the yield of the reaction product is low. The purification process to separate the product from the unreacted porphyrin also involves tedious chromatographic separation. To overcome this, on some occasions, a very large excess of the metal source has been used. Thus, none of the above methods can be considered as a convenient atom-conserved method for the preparation of molybdenum and tungsten porphyrins.

To overcome these, we report a one-pot strategy to synthesize metalloporphyrins in very good yield. Such a reaction was carried out in an organic melt like benzoic acid as the matrix in a solid-state reaction (Scheme 1).[10] Heating a mixture of 5,10,15,20-*meso*-tetraphenylporphyrin (H_2TPP) and an equivalent amount of $[M(NO)_2py_2Cl_2]$ (M = Mo, W) in a benzoic acid melt affords the formation of metalloporphyrins in quantitative yield.

The synthesized complexes are isolated as $[Mo^{V}O(TPP)(OOCPh)]$ (**1**) and $[W^{V}O(TPP)(OOCPh)]$ (**2**). These complexes are characterized by different spectroscopic techniques, electrochemical studies, and single-crystal X-ray diffraction analysis. The reactivity of **1** and **2** toward benzenethiol under aerobic as well as anaerobic conditions is also studied.

Received: April 23, 2012
Published: May 23, 2012

   dx.doi.org/10.1021/ic3008377 | *Inorg. Chem.* 2012, 51, 6412−6420

Scheme 1. Reaction Scheme for the Incorporation of Molybdenum and Tungsten inside the Porphyrin Core

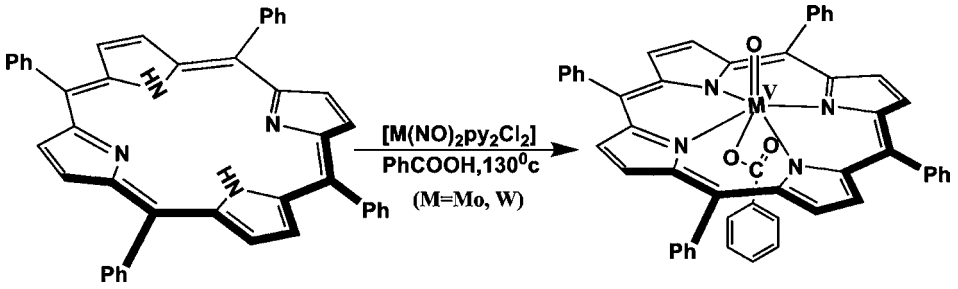

EXPERIMENTAL SECTION

Materials. Ammonium heptamolybdate, sodium tungstate, hydroxylamine hydrochloride, benzaldehyde, and thiophenol were obtained from S. D. Fine Chemicals Ltd., India, and benzoic acid was obtained from Loba Chemie, India. Pyrrole was obtained from Aldrich. Distilled water was used to wash the crude product, and solvents like acetic acid, pyridine, propionic acid, benzene, toluene, dichloromethane (DCM), dimethylformamide (DMF), methanol, and petroleum ether (60−80 °C) were obtained from Thomas Baker, India, and distilled prior to use by standard procedures. $[Mo(NO)_2py_2Cl_2]$ and $[W(NO)_2py_2Cl_2]$ were prepared following the procedure reported earlier.[11] Free-base porphyrin ($TPPH_2$) was prepared following the Adler method.[12]

Physical Methods. Elemental analyses for carbon, hydrogen, and nitrogen were obtained with a Perkin-Elmer 2400 microanalyzer. IR spectra were recorded on a Bruker Vertex 70 Fourier transform IR (FTIR) spectrophotometer with pressed KBr disks. Electronic absorption spectral measurements were carried out with a Perkin-Elmer (Lambda 35) spectrophotometer. Electrospray ionization mass spectrometry (ESI-MS) spectra were recorded on a Waters-Q-Tof Premier-HAB213 spectrometer. The ESI-MS capillary was set at 3.5 kV, and the cone voltage was 10 V. The mass spectral peaks were comprised of isotopic distribution, and only the central strong line is reported. ^{1}H NMR spectroscopic measurements for magnetic moment calculation of the complexes were recorded with a JEOL-500 NMR spectrometer. From solvent−proton splitting, the effective magnetic moment (μ_{eff}) values of the complexes were determined by following the Evans method.[13] X-band electron spin resonance (ESR) measurements were carried out in toluene at room temperature and also at 120 K on a Bruker EMX spectrometer. Cyclic voltammetry and differential pulse polarography (DPP) measurements were made with BASi Epsilon, EC Bioanalytical Systems, Inc. Cyclic voltammograms of 10^{-3} M solutions of the compounds were recorded with a glassy carbon electrode as the working electrode, 0.2 M Bu_4NClO_4 as the supporting electrolyte, Ag/AgCl as the reference electrode, and platinum as the auxiliary electrode in DCM. All electrochemical experiments were done under an argon atmosphere at 298 K. Potentials were referenced against internal ferrocene (Fc) and are reported relative to the Ag/AgCl electrode [$E_{1/2}(Fc^+/Fc)$ = 0.459 V vs Ag/AgCl electrode].

The crystals used in the analyses were glued to glass fibers and mounted on a Bruker SMART APEX diffractometer. The instrument was equipped with a CCD area detector, and data were collected using graphite-monochromated Mo Kα radiation (λ = 0.71069 Å) at low temperature (100 K). Cell constants were obtained from the least-squares refinement of three-dimensional centroids through the use of CCD recording of narrow ω-rotation frames, completing almost all-reciprocal space in the stated θ range. All data were collected with *SMART 5.628* (Bruker, 2003) and were integrated with the Bruker *SAINT* program.[14] An empirical absorption correction was applied to the collected reflections with *SADABS*[15] using *XPREP*.[16] The structure was solved using *SIR97*[17] and refined using *SHELXL-97*.[18] Full-matrix least-squares difference Fourier cycles were performed and located the non-hydrogen atoms. Only a few hydrogen atoms could be located in the difference Fourier maps in each structure. The rest were placed in calculated positions using idealized geometries and assigned fixed isotropic displacement parameters. All non-hydrogen atoms were refined with anisotropic displacement parameters unless otherwise stated.

Computational Details. All calculations were performed at the level of density functional theory (DFT)[19] by employing a B3LYP[20] hybrid functional using the *Gaussian 03* program.[21] Molecular orbitals were visualized using G View. The 6-31g+(d,p) basis set was used for the carbon, hydrogen, nitrogen, and oxygen atoms, and the effective core potential basis set LANL2DZ was used for the molybdenum and tungsten atoms. The geometry of the complexes was taken from the crystal structure.

Synthesis. *Synthesis of Benzoato(5,10,15,20-meso-tetraphenylporphyrinato)oxomolybdenum(V) (**1**).* In a typical experiment, 500 mg of H_2TPP and an equivalent amount of $[Mo(NO)_2py_2Cl_2]$ (~314 mg) were mixed in 10 g of benzoic acid and ground well in a mortar. The whole mass was then taken in a 16-cm-long B-24 test tube. Argon was purged through the mixture for 1 h, and the mass was then melted at around 130 °C for 1 h, cooled, and leached with boiling water to remove excess benzoic acid. The product was then dissolved in toluene and dried over anhydrous Na_2SO_4, and then the toluene solution was evaporated to dryness in a rotary evaporator to obtain a green solid. The solid was recrystallized from DCM and petroleum ether (60−80 °C) to yield dark-green, block-shaped, diffraction-quality crystals. Yield: 96%. Molecular formula: $C_{51}H_{33}N_4O_3Mo$. Molecular mass: 847.16. Elem anal Calcd (found) for $C_{51}H_{33}N_4O_3Mo$: C, 72.42 (72.33); H, 3.93 (4.14); N, 6.62 (6.23). UV−vis [CH_2Cl_2; λ_{max} (log ε)]: 339 (4.89), 414 (sh), 483 (5.10), 608 (4.33), 652 (4.20). FTIR (KBr disk, cm^{-1}): 940 ($\nu_{Mo=O}$). ESR (in toluene): at room temperature, $\langle g\rangle$ = 1.967 (central line) for the complexes with molybdenum, and I = 0 with six hyperfine lines for I = $^5/_2$ (A_{iso} = 40.18 G); the central line splits into nine superhyperfine lines because of the coordinated four nitrogen nuclei of the porphyrin (A_{iso} = 2.37 G); at 120 K: $g_{\|}$ = 1.9754, $A_{\|}$ = 23.53, $g_{\perp}$ = 1.9678, $A_{\perp}$ = 24.30). ESI-MS (m/z): 847.14 ($[M]^+$), 726.12 ($[M$ − benzoate$]^+$). Solution magnetic moment (by the Evans method): μ_{eff} = 1.61 μ_B in DMF.

*Synthesis of Benzoato(5,10,15,20-meso-tetraphenylporphyrinato)oxotungsten(V) (**2**).* Following the similar procedure as that mentioned for **1**, the tungsten analogue was prepared using $[W(NO)_2py_2Cl_2]$ as the tungsten metal source. This was stoichiometrically mixed with H_2TPP with a sufficient excess of benzoic acid and powdered, and the mixture was allowed to heat at 130 °C under a blanket of argon for 9 h and cooled. The solid was washed with hot water to remove excess benzoic acid and finally extracted by toluene. The toluene extract was dried over dry Na_2SO_4, and then the toluene was removed over a rotary evaporator to yield the product. The solid was recrystallized from DCM, methanol, and petroleum ether (60−80 °C) to yield purple, block-shaped, diffraction-quality crystals. Yield: 94%. Molecular formula: $C_{51}H_{33}N_4O_3W$. Molecular mass: 933.17. Elem anal. Calcd (found) for $C_{51}H_{33}N_4O_3W$: C, 65.61 (64.92); H, 3.56 (4.06); N, 6.00 (5.74). UV−vis [CH_2Cl_2; λ_{max} (log ε)]: 455 (5.23), 588 (3.83), 630 (3.61). FTIR (KBr disk, cm^{-1}): 949 ($\nu_{W=O}$). ESR (in toluene): central line $\langle g\rangle$ = 1.882 for the complexes with I = 0 with two less intense lines for I = $^1/_2$ (A_{iso} = 45.37 G; at room temperature), and g_1 = 1.9054, g_2 = 1.8759, g_3 = 1.8529, and $\langle g\rangle$ = 1.8780 (at 120 K). ESI-MS (m/z):

dx.doi.org/10.1021/ic3008377 | *Inorg. Chem.* 2012, 51, 6412−6420

Scheme 2. Proposed Steps Involved in the Formation of 3 and 4 (See the Text)

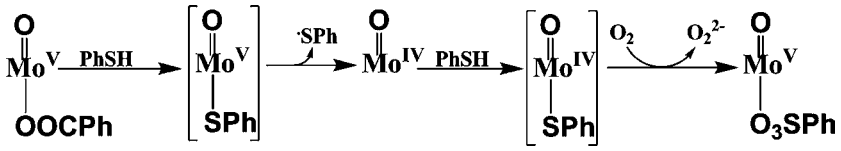

933.17 ([M]$^+$), 812.16 ([M − benzoate]$^+$). Solution magnetic moment (by the Evans method): μ_{eff} = 1.43 μ_B in DMF.

Synthesis of (5,10,15,20-meso-Tetraphenylporphyrinato)-oxomolybdenum(IV) (3). A total of 20 mg of **1** was dissolved in 30 mL of toluene in a 50 mL round-bottomed flask. The solution was air freed by purging with argon for 1 h, and an excess of benzenethiol (~0.3 mL) was added to the solution. The color of the solution immediately changed from green to red. Argon-purged petroleum ether (60−80 °C) was added slowly to layer the red solution, and the container was allowed to stand at 4 °C. After 5 days, block-shaped red crystals appeared that were washed with petroleum ether and dried in vacuum. Some of these crystals were found to be suitable for single-crystal X-ray diffraction. Yield: 78%. Molecular formula: $C_{44}H_{28}N_4O_1Mo$. Molecular mass: 726.13. Elem anal. Calcd (found) for $C_{44}H_{28}N_4O_1Mo$: C, 72.93 (72.96); H, 3.89 (3.91); N, 7.73 (7.74). UV−vis [CH_2Cl_2; λ_{max} (log ε)]: 429 (5.34), 556 (4.09), 596 (3.34). FTIR (KBr disk, cm^{-1}): 979 ($\nu_{Mo=O}$). ESI-MS (m/z): 726.13 ([M]$^+$).

Synthesis of Benzenesulfonato(5,10,15,20-meso-tetraphenylporphyrinato)oxomolybdenum(V) (4). A total of 20 mg of **1** was dissolved in 10 mL of DCM in a round-bottomed flask. A total of 0.3 mL of benzenethiol was added, and the solution was allowed to stand overnight in air. The initial green color of **1** changed to red because of the formation of **3**, and this subsequently changed to brownish green with time. A total of 10 mL of petroleum ether (60−80 °C) was added to the solution. Slow evaporation of the solvents led to dark-green, needle-shaped crystals of **4** appearing on the surface of the flask within a few days. These crystals were washed with hexane to remove excess benzenethiol. Yield: 89%. Molecular formula: $C_{50}H_{33}N_4O_4S_1Mo$. Molecular mass: 883.13. Elem anal. Calcd (found) for $C_{50}H_{33}N_4O_4S_1Mo$: C, 68.10 (68.97); H, 3.77 (3.71); N, 6.35 (6.39). UV−vis [CH_2Cl_2; λ_{max} (log ε)]: 342 (4.97), 416 (sh), 487 (5.016), 614 (4.31), 657 (4.21). FTIR (KBr disk, cm^{-1}): 956 ($\nu_{Mo=O}$). ESI-MS (m/z): 883.13 ([M]$^+$), 726.12 ([M − O_3SPh]$^+$). ESR (in toluene): at room temperature, $\langle g \rangle$ = 1.969 (central line) for the complexes with molybdenum, and I = 0 with six hyperfine lines for I = $^5/_2$ (A_{iso} = 41.23G); the central line splits into nine superhyperfine lines because of the coordinated four nitrogen nuclei of the porphyrin (A_{iso} = 2.38 G); at 120 K, $g_{||}$ = 1.9772, $A_{||}$ = 24.55, $g_{\perp}$ = 1.9683, and $A_{\perp}$ = 25.32. Solution magnetic moment (by the Evans method): μ_{eff} = 1.56 μ_B in DMF.

RESULTS AND DISCUSSION

Synthesis. The methodologies reported in the literature for the synthesis of molybdenum and tungsten porphyrins are all in solution. A new strategy introduced here is related to the reaction of a complex of the metal source and porphyrin at high temperature for which a relatively less reactive organic compound like benzoic acid is identified to provide the matrix to melt above 100 °C. The choice of the metal source as $[M(NO)_2py_2Cl_2]$ (M = Mo, W) has been done because the byproducts in the reaction are NO, HCl, and pyridine and their reaction products are all volatile in nature; therefore, the purity of the product is ensured. Almost quantitative yield of the product has been achieved by this methodology. On the basis of molybdenum and tungsten complexes, the products were isolated as **1** and **2**, respectively. Such a reaction proceeds well using $M(CO)_6$ (M = Mo, W) as the starting material, but the reaction has to be carried out in a sealed tube to prevent sublimation of the carbonyl compound under open conditions. It is interesting to note that, in the starting complex $[M(NO)_2py_2Cl_2]$, the formal oxidation state of the metal is zero because of the presence of two linear M−N−O bonds thus bearing the charge on nitric oxide as NO$^+$. Under open conditions in argon, we found the release of pyridine, HCl, and NO. The nitrosyl groups on thermal dissociation may gain electrons from the metal to form neutral NO, leaving the metal formally in the M^{II} oxidation state. This could led to the formation of reactive [M(TPP)], which should have ultimately dimerized to form the quadruple-bonded $[M_2(TPP)_2]$. The absence of finding such a metal−metal-bonded species can be explained by invoking the oxidation of quadruple-bonded $\{M^{II}\}_2$ in the presence of the byproduct HCl, and such a reaction is known.[22] Once the metal gets partially oxidized, the overall stability of the TPP-coordinated metal being an avid oxo acceptor would attract an oxo group available from the trace amount of air. This leads to a stable hexacoordinated species by coordination of the benzoate group trans to the oxo group. At the next stage, substitution of the benzoate axial ligand can be achieved. When a molecule like thiophenol, which is also a mild reducing agent, is used, it substitutes the benzoate group under anaerobic conditions. The formation of [Mo^{IV}O(TPP)] (**3**)[23] follows first the coordination of thiolate, followed by an intramolecular redox reaction across Mo^V−SPh.

However, in the presence of excess benzenethiol, the molybdenum(IV) species gets coordinated to the SPh$^-$ group, and in air, the reaction between **1** and benzenethiol finally leads to the formation of [Mo^{V}O(TPP)(O_3SPh)] (**4**)[24] via the intermediate **3**. **3** upon coordination of SPh reacts by aerial oxidation to generate peroxide, which, in turn, oxidizes thiophenolate to benzenesulfonate to form **4** (see Scheme 2).[25] It is important to note that benzenethiol with aerial oxidation is slowly oxidized to diphenyl disulfide only.[26] Faster oxidation up to this stage can be achieved in the presence of a base or an oxidizing agent like iodine.[27] The oxidation of benzenethiol to diphenyl disulfide by complex **1** is reminiscent of a similar reaction achieved by chromium(V) corrole, leading to the reduction of Cr^V to Cr^{IV}.[28] In the present case, we could isolate and structurally characterize the molybdenum(IV) complex **3**. Oxidation beyond disulfide to benzenesulfonate is thus a hitherto unknown oxidation reaction catalyzed by the metal porphyrin frame. A similar reduction of aerial oxygen by xanthine oxidase is known. The formation of any intermediate like a superoxide radical could not be identified by monitoring the reaction by ESR and also by a monoformazan test using nitroblue tetrazolium (NBT). The addition of a NBT solution prepared in an aqueous phosphate buffer to the reaction medium does not show any generation of a blue color in the aqueous layer, confirming the absence of superoxide formation in the reaction medium. **2** undergoes similar chemistry albeit very slowly. This is in accordance with the kinetically sluggish behavior of any tungsten analogue of molybdenum.

X-ray Structure. Complexes **1**−**4** are structurally characterized by single-crystal X-ray diffraction analysis. Suitable

dx.doi.org/10.1021/ic3008377 | Inorg. Chem. 2012, 51, 6412−6420

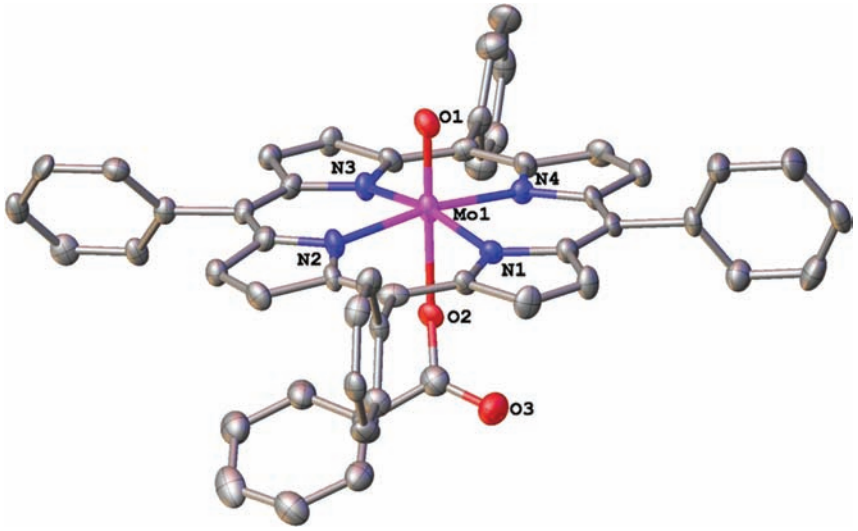

Figure 1. Perspective view of **1** in 50% probability thermal ellipsoids (hydrogen atoms are omitted for clarity). Selected bond distances: Mo1−O1 = 1.712(5) Å; Mo1−O2 = 2.090(5) Å.

Table 1. Crystallographic Data for 1−4

	1	2	3	4
empirical formula	$C_{51}H_{33}N_4O_3Mo$	$C_{51}H_{33}N_4O_3W$	$C_{44}H_{28}N_4O_1Mo$	$C_{50}H_{33}N_4O_4S_1Mo$
fw	845.75	933.66	726.12	881.80
cryst color	dark green	purple	red	dark green
temp (K)	100(5)	100(5)	100(5)	100(5)
radiation	Mo Kα	Mo Kα	Mo Kα	Mo Kα
wavelength (Å)	0.71069	0.71069	0.71069	0.71069
cryst syst	triclinic	triclinic	tetragonal	monoclinic
space group	$P\bar{1}$	$P\bar{1}$	$I4/m$	$P2_1/n$
a (Å)	10.300(5)	10.341(5)	13.328(5)	13.516(5)
b (Å)	11.185(5)	11.124(5)	13.328(5)	12.576(5)
c (Å)	17.380(5)	17.438(5)	9.624(5)	23.980(5)
α (deg)	87.880(5)	87.777(5)	90	90
β (deg)	79.550(5)	79.837(5)	90	103.875(5)
γ (deg)	77.144(5)	77.322(5)	90	90
volume (Å^3)	1919.7(14)	1926.3(14)	1709.6(13)	3957(2)
Z	2	2	2	4
d_{calcd} (g/cm^3)	1.463	1.610	1.408	1.480
μ (mm^{-1})	0.394	3.051	0.425	0.438
F(000)	866	930	740	1804
θ range (deg)	2.21−25.50	1.88−25.50	2.16−25.46	2.24−25.50
reflns collected	10342	10316	4549	20800
indep reflns	7003	7008	848	7334
$R_{int.}$	0.0535	0.0295	0.0435	0.0898
GOF	1.114	1.162	1.424	1.031
final Rindices $[I > 2\sigma(I)]^a$	R1 = 0.0805, wR2 = 0.1901	R1 = 0.0588, wR2 = 0.1545	R1 = 0.0600, wR2 = 0.1421	R1 = 0.0702, wR2 = 0.1674
R indices (all data)^a	R1 = 0.1187, wR2 = 0.2490	R1 = 0.0712, wR2 =0.1805	R1 = 0.0613, wR2 = 0.142	R1 = 0.1137, wR2 = 0.2158

^{a}R1 = $\sum||F_o| - |F_c||/\sum|F_o|$. wR2 = $\{\sum[w(F_o^2 - F_c^2)^2]/\sum[w(F_o^2)^2]\}^{1/2}$.

diffraction-quality single crystals were obtained from the crystallization procedures described earlier.

Solid-State Structure of 1. The molecular structure of **1** is presented in Figure 1. Single-crystal X-ray diffraction analysis revealed that **1** comprises neutral **1** and crystallizes in a triclinic crystal system with space group $P\bar{1}$. The terminal metal−oxo bond distance is 1.712(5) Å, and the metal−oxygen bond distance from benzoate coordination is 2.090(5) Å. The central molybdenum atom has distorted octahedral geometry and is displaced toward the terminal metal−oxo by a distance of 0.205 Å from the mean plane of the porphyrin nitrogen atoms. A summary of the crystallographic data and structure analysis is given in Table 1.

Solid-State Structure of 2. **2** shows an X-ray structure very similar to that of **1**, with the terminal metal−oxo and metal−oxygen bond distances from benzoate coordination being 1.724(6) and 2.061(6) Å, respectively. Interestingly, in this case also the out-of-plane displacement of the metal toward the terminal oxo is 0.205 Å. The molecular view of complex **2** is shown in Figure 2.

dx.doi.org/10.1021/ic3008377 | *Inorg. Chem.* 2012, 51, 6412−6420

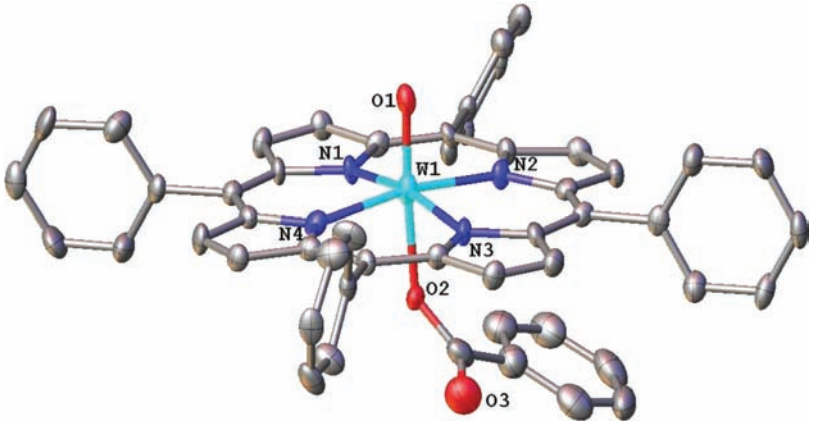

Figure 2. Perspective view of **2** in 50% probability thermal ellipsoids (hydrogen atoms are omitted for clarity). Selected bond distances: W1−O1 = 1.724(6) Å; W1−O2 = 2.061(6) Å.

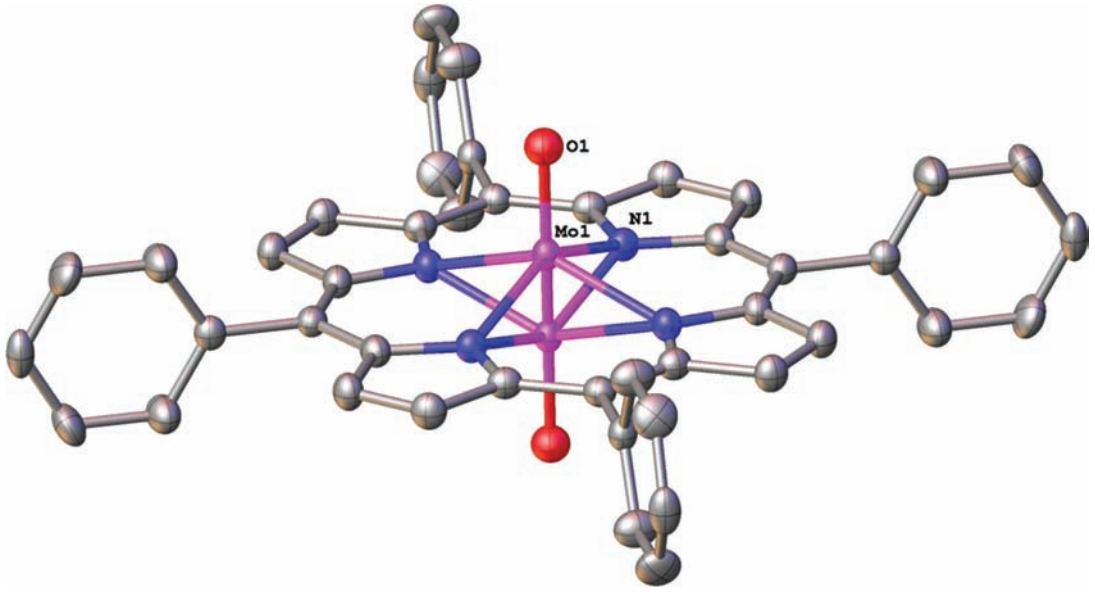

Figure 3. Perspective view of **3** in 50% probability thermal ellipsoids as obtained from single-crystal X-ray diffraction analysis (hydrogen atoms are omitted for clarity). The Mo═O moiety is disordered 50−50 above and below the N_4 plane. Selected bond distance: Mo1−O1 = 1.694(12) Å.

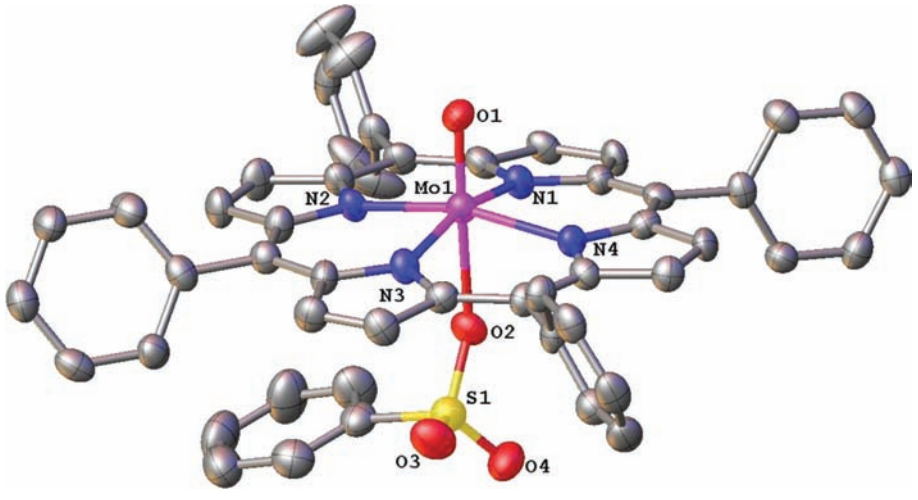

Figure 4. Perspective view of molecule **4** in 50% probability thermal ellipsoids (hydrogen atoms are omitted for clarity). Selected bond lengths: Mo1−O1 = 1.664(4) Å; Mo1−O2 = 2.188(4) Å.

dx.doi.org/10.1021/ic3008377 | *Inorg. Chem.* 2012, 51, 6412−6420

Solid-State Structure of 3. The molecular view of **3** is shown in Figure 3. Single-crystal X-ray diffraction analysis revealed that the complex crystallizes in a tetragonal crystal system with space group $I4/m$. The asymmetric unit consists of one-fourth of the molecule. The terminal metal−oxo distance is 1.693(12) Å. The central molybdenum atom has a square-pyramidal geometry and is displaced from the mean plane of the porphyrin nitrogen atoms by a distance of 0.645 Å toward the terminal metal−oxo. The Mo═O moiety is disordered 50−50 above and below the N_4 plane.

Solid-State Structure of 4. The molecular view of **4** is shown in Figure 4. It crystallizes in a monoclinic crystal system with space group $P2_1/n$. The terminal metal−oxo bond distance is 1.664(4) Å, and the molybdenum metal−oxygen bond distance from benzenesulfonate is 2.188(4) Å. The metal-ion displacement toward the terminal metal−oxo is 0.291 Å. Among **1**−**4**, the metal-ion displacement from the N_4 basal plane of porphyrin has been found to be a maximum for the pentacoordinated complex **3**, and for the rest, which are hexacoordinated complexes, this displacement is much less, as expected.

UV−Vis Spectroscopy. UV−vis absorption maxima and molar absorptivity in DCM of these complexes are summarized in the Experimental Section. Upon the addition of excess thiophenol to the green solution of **1**, it immediately changes to red, showing a red shift of both the Soret and Q bands, as shown in Figure 5. Similar spectral changes are also observed

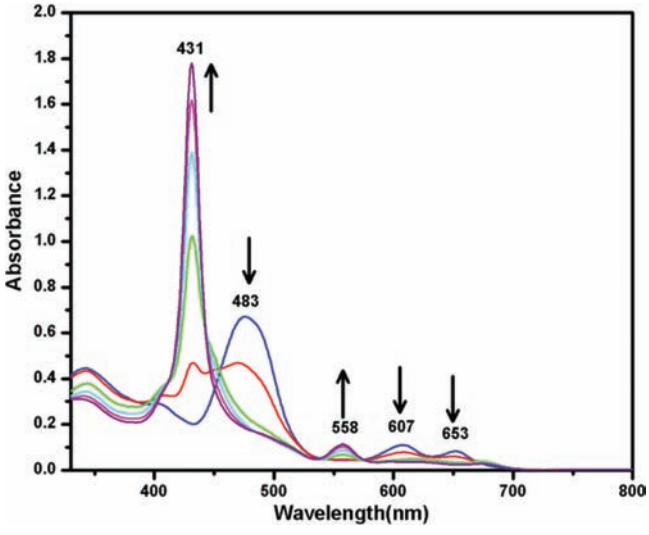

Figure 5. Electronic spectral changes of **1** (blue) in excess benzenethiol in toluene.

for **2** (Figure 6). Because of the kinetically slow reaction of the tungsten compound, the formation of the intermediate species $[W^{V}O(TPP)(SPh)]$ is clearly observed, in this case with the appearance of a band at 464 nm.

IR Spectroscopy and ESI-MS. The FTIR spectra of these complexes displayed strong absorption bands at around 940−980 cm^{-1}, which are well-known for ν(M═O), showing the complexes as metal−oxo porphyrins. In the ESI-MS spectrum of **1**, **2**, and **4** in methanol, the molecular ion peak (m/z with isotropic distribution) could be observed as a low intense peak. However, the most intense peak corresponds to the respective m/z value of these complexes appearing with the loss of the axial ligand, suggesting its weak attachment. The ESI-MS

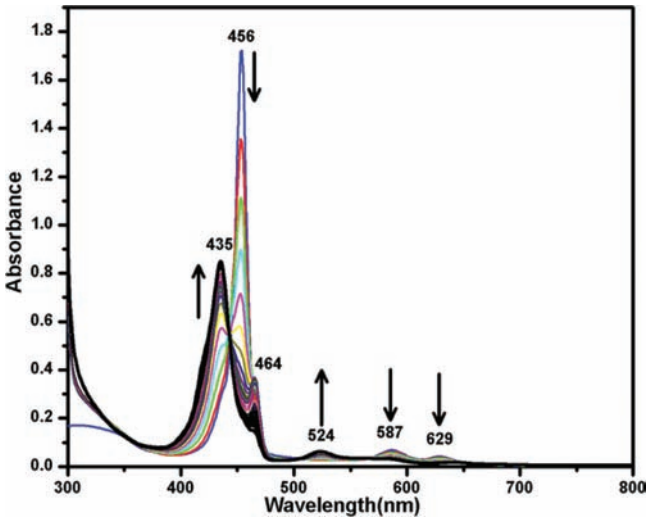

Figure 6. Electronic spectral changes in 16 h of **2** (blue) after the addition of excess benzenethiol in toluene. The band at 464 nm is indicative of the intermediate species $[W^{V}O(TPP)(SPh)]$.

spectrum of **3** shows the $[M + 1]^+$ peak at the calculated m/z value with excellent isotropic distribution.

Electrochemistry. The cyclic voltammograms of **1** and **2** in DCM are displayed in Figure 7. Complex **2** shows three

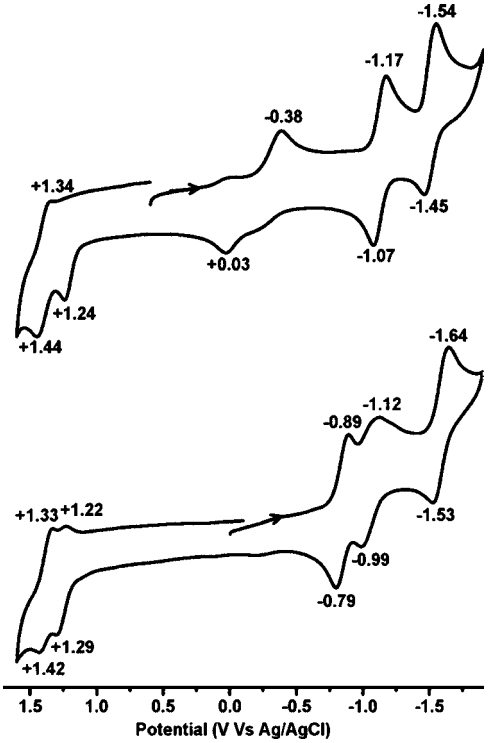

Figure 7. Cyclic voltammograms of **1**(above) and **2** (below) in DCM containing 0.2 M TBAP at a scan rate of 0.1 V/s.

reversible reductions at $E_{1/2}$ = −0.84, −1.05, and −1.58 V vs Ag/AgCl. The first reduction involves a W^{V}/W^{IV} process.[7] The other two reductions are porphyrin-based to yield porphyrin π-anion radical and dianion, respectively.[29] For **1**, the metal reduction process (Mo^{V}/Mo^{IV}) is irreversible[30] with E_{pc} at +0.38 V vs Ag/AgCl. This electrochemical observation clearly supports the unstable nature of $[Mo^{IV}O(TPP)(X)]$ (X =

dx.doi.org/10.1021/ic3008377 | Inorg. Chem. 2012, 51, 6412−6420

−OOCPh or −SPh), which is stabilized by elimination of the axial ligand trans to the oxo group. The metal−oxygen bond from benzoate coordination in **2** is about 0.03 Å shorter than that in **1**. This implicates stronger coordination of the benzoate ion to the tungsten center, which helps tungsten retain its geometry during the reduction process, reflecting the reversible nature of the process. The lower potential value for metal reduction also suggests that oxomolybdenum(IV) porphyrin can be achieved easily from **1** by chemical means. Thus, **1** with a mild reducing agent like benzenethiol in the absence of air is immediately converted to an oxomolybdenum(IV) porphyrin complex as described in the Experimental Section.

Using tetrabutylammonium benzoate (TBAB) as the supporting electrolyte, the metal-centered redox process of **1** becomes quasi-reversible (Figure 8) and shows only one wave

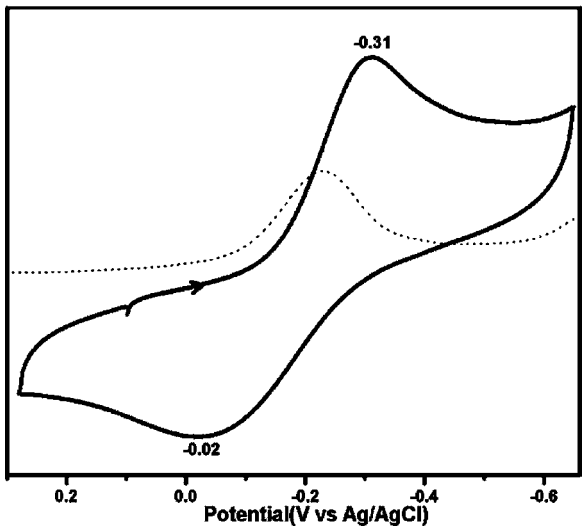

Figure 8. Metal redox process of **1** in DCM containing 0.2 M TBAB at a scan rate of 0.1 V/s.

in DPP measurement compared with the appearance of two waves when tetrabutylammonium perchlorate (TBAP) is used (Figure 9). This supports coordination of the perchlorate ion in the reoxidation process, as shown in Scheme 3.

When excess thiophenol was added to the solution of **1**, the current height for the irreversible metal reduction ($Mo^{V} \rightarrow Mo^{IV}$) of **1** at E_{pc} = −0.38 V decreases and a reversible wave starts to generate around $E_{1/2}$ = +0.09 V for Mo^{IV}/Mo^{V} oxidation of complex **3** (see the Supporting Information).

The cyclic voltammogram of **4** shows features very similar to those of **3** (Figure 10).[31] The only difference is that the metal redox process in **3** involves $Mo^{IV} \rightarrow Mo^{V}$ oxidation, while for **4**, it is a reduction process ($Mo^{V} \rightarrow Mo^{IV}$). The similar nature of the voltammograms may be due to the weak coordination of the benzenesulfonate ion to the molybdenum center [Mo−O = 2.188(4) Å], as in the case of the perchlorate-coordinated complex.[31]

ESR Spectroscopy. Solution ESR spectra of **1** and **4** show typical Mo^{V} signals for molybdenum (75%, I = 0) complexes with g_{iso} values $\langle g \rangle$ = 1.967 and 1.969, respectively, with six hyperfine lines ($A_{iso} \approx 41$ G) for ^{95,97}Mo ($I = {}^{5}/_{2}$). Superhyperfine lines ($A_{iso} \approx 2.4$ G) due to the coordinated four nitrogen atoms from the porphyrin macrocycle are observed. For **2**, $\langle g \rangle$ = 1.882, with two hyperfine lines, A_{iso} = 45.37 G, for tungsten appearing. The superhyperfine

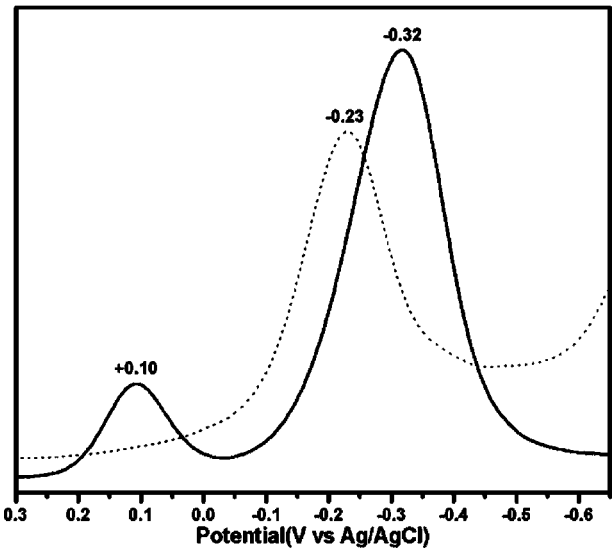

Figure 9. Comparison of the metal redox process (DPP) of **1** in DCM using TBAP (solid line) and TBAB (dotted line) as supporting electrolytes.

interaction from the porphyrin nitrogen atoms could not be resolved, suggesting different electronic interaction compared with its molybdenum analogue.

Frozen ESR spectra of these complexes are anisotropic in nature. Complexes **1** and **4** have similar ESR spectra with $g_{\|}$ values of 1.9754 and 1.9772 and with $g_{\perp}$ values of 1.9678 and 1.9683, respectively. The ESR spectrum of **2** is rhombic in nature, showing three distinct g values (see the Supporting Information).

Solution Magnetic Behavior. From solvent−proton splitting, the effective magnetic moment (μ_{eff}) values of the complexes are determined by the Evans method in DMF. The μ_{eff} values of 1.61, 1.43, and 1.56 μ_B for **1**, **2**, and **4**, respectively, are slightly lower than the spin-only value (4d or 5d metal with orbital contribution) and are in good agreement with a d^1 electronic configuration of the complexes. Complex **3** is diamagnetic, and no solvent−proton splitting was observed, as expected.

DFT Calculations. Close inspection of the molecular orbitals of **1** and **2** as obtained from DFT level calculations indicate that the highest occupied molecular orbital (HOMO) involves the metal d_{xy} orbital predominantly with 87.31% and 91.30% metal contribution for **1** and **2**, respectively. The small difference arises mainly from the contributions from nitrogen orbitals (total contribution = 3.95%) in the case of **1**. However, the HOMO−1 orbital of **1** is built up with both the metal and ligand orbitals compared to **2**, which is totally ligand-based (Figure 11). This makes a difference in the electronic population, reflecting the superhyperfine interaction in the ESR spectrum of **1**. For **2**, the absence of such metal d orbital and ligand orbital interactions justifies the absence of any superhyperfine interaction.

CONCLUSION

In summary, we have synthesized molybdenum(V) and tungsten(V) porphyrin complexes by a new synthetic route in almost quantitative yield. This method is a general method, and other metalloporphyrins can be synthesized with high yield. These hexacoordinated complexes readily respond to ligand substitution trans to the oxo group, and when mild reducing

dx.doi.org/10.1021/ic3008377 | Inorg. Chem. 2012, 51, 6412−6420

Scheme 3. Electrochemical Processes of 1 and 2

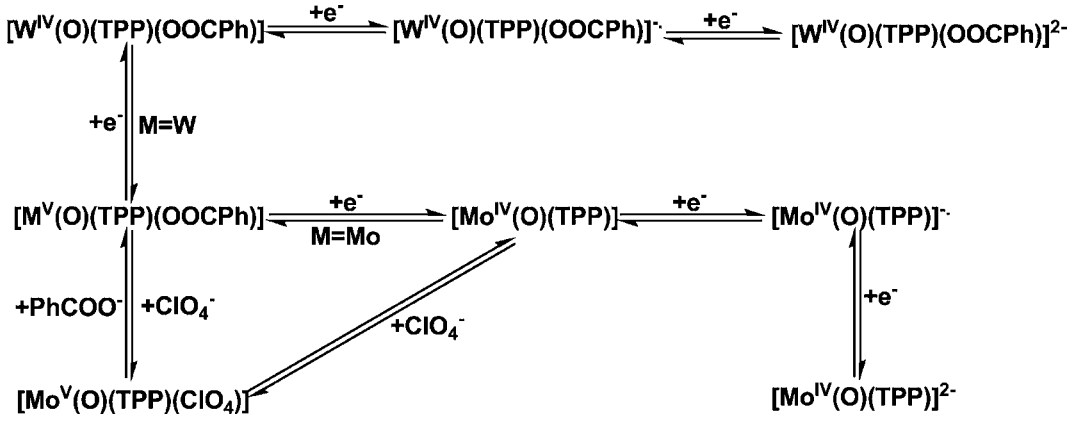

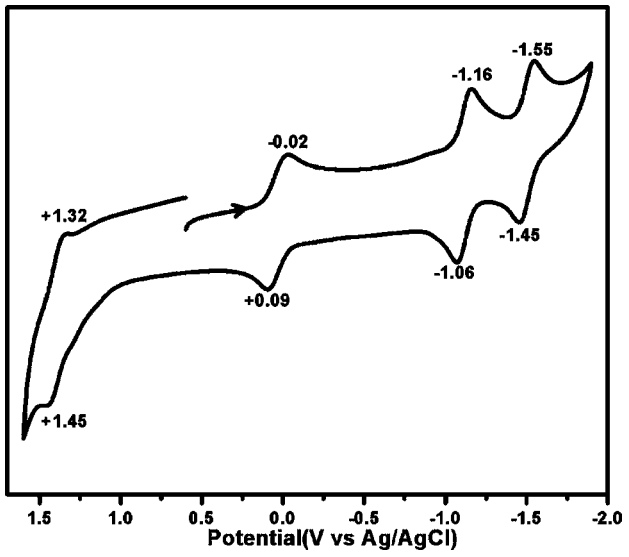

Figure 10. Cyclic voltammograms of 4 in DCM containing 0.2 M TBAP at a scan rate of 0.1 V/s.

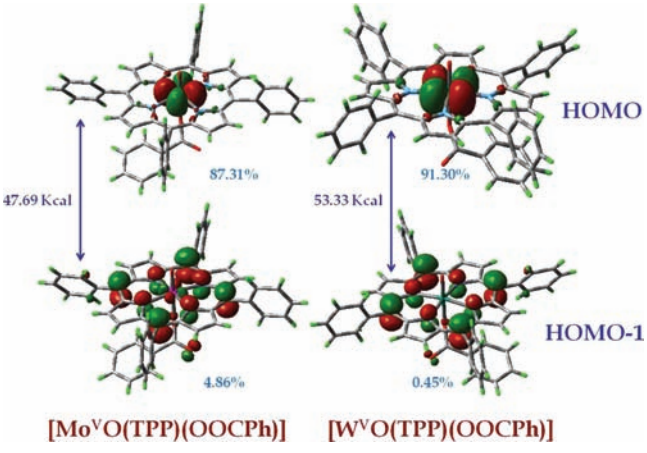

Figure 11. Frontier orbital plots of 1 and 2.

benzenethiolate is coordinated, the intramolecular electron transfer leads to the reduction of Mo^{V} to Mo^{IV} concomitant to the oxidation of benzenethiol to disulfide. However, in air the Mo^{IV} formed activates the molecular oxygen to peroxide and the reaction proceeds further with the ultimate oxidation of benzenethiolate to benzenesulfonate. This reaction does not occur by simple aerial oxidation,[32] while here such an oxidation is possible because of the catalyzing role of molybdenum(IV) porphyrin present in the reaction mixture.

■ ASSOCIATED CONTENT

Ⓢ Supporting Information

Synthesis of $[M(NO)_2py_2Cl_2]$, X-ray crystallographic files (in CIF format), electronic, MS, FTIR, and ESR spectra, a cyclic voltammogram, and crystal packing diagrams of **1**–**4**. This material is available free of charge via the Internet at http://pubs.acs.org.

■ AUTHOR INFORMATION

Corresponding Author

*E-mail: abya@iitk.ac.in.

Notes

The authors declare no competing financial interest.

■ ACKNOWLEDGMENTS

G.N. acknowledges Doctoral Research Fellowships from the CSIR, New Delhi, India, and S.S. thanks the DST, New Delhi, India, for funding the project.

■ REFERENCES

(1) Campbell, W. M.; Burrell, A. K.; Officer, D. L.; Jolley, K. W. *Coord. Chem. Rev.* **2004**, 1363–1379 and references cited therein.

(2) (a) Sternberg, E. D.; Dolphin, D.; Brückner, C. *Tetrahedron* **1998**, *54*, 4151–4202 and references cited therein. (b) Mody, T. D. *J. Porphyrins Phthalocyanines* **2000**, *4*, 362–367. (c) MacDonald, I. J.; Dougherty, T. J. *J. Porphyrins Phthalocyanines* **2001**, *5*, 105–129.

(3) (a) Rothemund, P.; Menotti, A. R. *J. Am. Chem. Soc.* **1948**, *70*, 1808–1812. (b) Dorough, G. D.; Miller, J. R.; Huennekens, F. M. *J. Am. Chem. Soc.* **1951**, *73*, 4315–4320. (c) Fleischer, E. B.; Lavallee, D. *J. Am. Chem. Soc.* **1967**, *89*, 7132–7133. (d) Adler, A. D.; Longo, F. R.; Kampas, F.; Kim., J. *J. Inorg. Nucl. Chem.* **1970**, *32*, 2443–2445. (e) Lindsey, J. S.; Woodford, J. N. *Inorg. Chem.* **1995**, *34*, 1063–1069.

(4) Kumar, A.; Maji, S.; Dubey, P.; Abhilash, G. J.; Pandey, S.; Sarkar, S. *Tetrahedron Lett.* **2007**, *48*, 7287–7290.

(5) Buchler, J. W.; Puppe, L.; Rohbock, K.; Schneehage, H. H. *Chem. Ber.* **1973**, *106*, 2710–2732.

(6) Srivastava, T. S.; Fleischer, E. B. *J. Am. Chem. Soc.* **1970**, *92*, 5518–5519.

(7) Newton, C. M.; Davis, D. G. *J. Magn. Reson.* **1975**, *20*, 446–457.

(8) (a) Luobeznova, I.; Raizman, M.; Goldberg, I.; Gross, Z. *Inorg. Chem.* **2006**, *45*, 386–394. (b) Nigel-Etinger, I.; Goldberg, I.; Gross, Z. *Inorg. Chem.* **2012**, *51*, 1983–1985.

(9) (a) Bains, M. S.; Davis, D. G. *Inorg. Chim. Acta* **1979**, *37*, 53–60. (b) Diebold, T.; Chevrier, B.; Weiss, R. *Inorg. Chem.* **1979**, *18*, 1193–

1200. (c) Imamura, T.; Numatatsu, T.; Terui, M.; Fujimoto, M. *Bull. Chem. Soc. Jpn.* **1981**, *54*, 170−174.
(10) Collman, J. P.; Garner, V. J. M.; Kim, K.; Ibers, J. A. *Inorg. Chem.* **1988**, *27*, 4513−4516.
(11) (a) Sarkar, S.; Subramanian, P. *Inorg. Chim. Acta* **1980**, *46*, L67−L68. (b) Sarkar, S.; Mohammad, I. B.; Subramanian, P. *Chem. Lett.* **1985**, *11*, 1633−1634.
(12) Adler, A. D.; Longo, F. R.; Finarelli, J. D.; Goldmacher, J.; Assour, J.; Korsakoff, L. *J. Org. Chem.* **1967**, *32*, 476.
(13) Evans, D. F. *J. Chem. Soc.* **1959**, 2003.
(14) *SAINT*$^{+}$, version 6.02; Bruker AXS: Madison, WI, 1999.
(15) Sheldrick, G. M. *SADABS, Empirical Absorption Correction Program*; University of Göttingen: Göttingen, Germany, 1996.
(16) *XPREP*, version 5.1; Siemens Industrial Automation Inc.: Madison, WI, 1995.
(17) Altomare, A.; Burla, M. C.; Camalli, M.; Cascarano, G. L.; Giacovazzo, C.; Guagliardi, A.; Moliterni, A. G. G.; Polidori, G.; Spagna, R. *J. Appl. Crystallogr.* **1999**, *32*, 115−119.
(18) Sheldrick, G. M. *SHELXL-97, Program for Crystal Structure Refinement*; University of Göttingen: Göttingen, Germany, 1997.
(19) Kohn, W.; Sham, L. J. *Phys. Rev.* **1965**, *140*, A1133−A1138.
(20) Becke, A. D. *Phys. Rev. A* **1988**, *38*, 3098−3100. (b) Becke, A. D.; Roussel, M. R. *Phys. Rev. A* **1989**, *39*, 3761−3767. (c) Lee, C.; Yang, W.; Parr, R. G. *Phys. Rev. B* **1988**, *37*, 785−789.
(21) Frisch, M. J.; et al. *Gaussian 03*; Gaussian, Inc.: Wallingford, CT, 2004.
(22) (a) Cotton, F. A.; Kalbacher, B. J. *Inorg. Chem.* **1976**, *15*, 522−524. (b) Bino, A.; Bursten, B. E.; Cotton, F. A.; Fang, A. *Inorg. Chem.* **1982**, *21*, 3755−3759.
(23) Diebold, T.; Chevrier, B.; Weiss, R. *Inorg. Chem.* **1979**, *18*, 1193−1200.
(24) Okubu, Y.; Okamura, A.; Imanishi, K.; Tachibana, J.; Umakoshi, K.; Sasaki, Y.; Imamura, T. *Bull. Chem. Soc. Jpn.* **1999**, *72*, 2241−2247.
(25) (a) Ledon, H. J.; Bonnet, M. *J. Am. Chem. Soc.* **1981**, *103*, 6209−6211. (b) Matsuda, Y.; Koshima, H.; Nakamura, K.; Murakami, Y. *Chem. Lett.* **1988**, *17*, 625−628. (c) Matsuda, Y.; Sakamoto, S.; Koshima, H.; Murakami, Y. *J. Am. Chem. Soc.* **1985**, *107*, 6415−6416.
(26) Witt, D. *Synthesis* **2008**, *16*, 2491−2509.
(27) Harnish, D. P.; Tarbell, D. S. *Anal. Chem.* **1949**, *21*, 968−969.
(28) Mahammed, A.; Gray, H. B.; Meier-Callahan, A. E.; Gross, Z. *J. Am. Chem. Soc.* **2003**, *125*, 1162−1163.
(29) Kadish, K. M.; Caemelbecke, E. V. *J Solid State Electrochem.* **2003**, *7*, 254−258.
(30) (a) Kadish, K. M.; Malinski, T.; Ledon, H. *Inorg. Chem.* **1982**, *21*, 2982−2987. (b) Suzuki, T.; Imamura, T.; Sumiyoshi, T.; Katayama, M.; Fujimoto, M. *Inorg. Chem.* **1990**, *29*, 1123−1129.
(31) Malinski, T.; Hanley, P. M.; Kadish, K. M. *Inorg. Chem.* **1986**, *25*, 3229−2335.
(32) (a) Evans, B. J.; Doi, J. T.; Musker, W. K. *J. Org. Chem.* **1990**, *55*, 2337−2344. (b) Ballistreri, F. P.; Tomaselli, G. A.; Toscano, R. M. *Tetrahedron Lett.* **2008**, *49*, 3291−3293.